International Journal of Chemistry, Mathematics and Physics (IJCMP)
[Vol-5, Issue-6, Nov-Dec, 2021]
https://dx.doi.org/10.22161/ijcmp.5.6.1
ISSN: 2456-866X

Structural and photoluminescence study of $SrAl_2O_4:Eu^{3+}$ phosphors synthesized by combustion method

P. J. Chaware, K. G. Rewatkar

Department of Physics, Dr. Ambedkar College, Nagpur, India

Received: 11 Oct 2021; Received in revised form: 03 Nov 2021; Accepted: 10 Nov 2021; Available online: 18 Nov 2021

Abstract— *The combustion synthesis method was employed for the synthesis of red-emitting monoclinic $SrAl_2O_4:Eu^{3+}$ phosphors. Structural characterization of annealed samples was carried out via X-ray Diffraction (XRD). XRD patterns reveal that strontium aluminate samples were cubic spinel nanoparticles and the grain size determined by the Debye-Scherrer formula is 35.34 nm. The vibrational stretching frequencies corresponding to the composites were confirmed by FT-IR spectroscopy. The PL spectra show the strongest emission at 612 nm corresponds to the $^5D_0 \rightarrow {}^7F_2$ transition of Eu^{3+}, which results in bright red color emitting phosphor used for display devices and lamp industries.*

***Keywords*— photoluminescence, strontium aluminate, XRD, FTIR.**

I. INTRODUCTION

Inorganic materials doped with rare earth ions have generated considerable interest in recent years due to their exceptional luminescent properties. Rare-earth doped phosphors have previously proved their utility in a variety of sectors, including illumination, radiation detection, medicinal applications, and solar energy consumption[1–3]. Alkaline earth aluminate, $SrAl_2O_4$, is one of the most important persistent luminescent compounds. Due to their high initial luminescent intensity and low-dimensional long afterglow property, strontium aluminate phosphors are an ideal material for widespread use in a variety of fields, including the dial plate of a glow watch, warning signs, escape routines, airports, buildings, and various types of ceramic materials, as well as textiles, and this could result in future nanoscale display devices [4–6].

Due to their amazing properties, such as safety, stability, and high quantum efficiency, strontium aluminates have been extensively investigated for use as phosphor host materials in a variety of applications. $SrAl_2O_4$ crystallises in two distinct crystallographic forms, with a reversible transition occurring at around 650°C. The low-temperature phase is monoclinic (space group P_{21}, a = 8.447 Å, b = 8.816 Å, c = 5.163Å and α= ϒ= 90º) [6–9], whereas the high-temperature phase has a hexagonal structure (space group $P6_3$). A three-dimensional framework of corner-sharing AlO_4 tetrahedrons forms the monoclinic $SrAl_2O_4$. Following that, the oxygen is shared with two aluminium ions, resulting in a net negative charge in each tetrahedron that is balanced by massive divalent cations that occupy two unique interstitial sites inside the tetrahedron framework. [10] .

The combustion synthesis method was employed in this study to produce $SrAl_2O_4$ phosphors doped with Eu3+ using urea as the fuel. X-ray diffraction (XRD) was utilized to assess the phase purity and structure of the phosphors as they were made. At room temperature, the photoluminescence characteristics of the resulting samples were analysed using a fluorescence spectrophotometer. The CIE chromaticity diagram was used to determine the CIE coordinates for the photoluminescent colour of nanophosphors. The FTIR technique is used to assess the existence of specific functional groups in a molecule.

II. EXPERIMENTAL

The $SrAl_2O_4:Eu^{3+}$ phosphors were synthesized using a combustion method. Strontium nitrate $[Sr(NO_3)_2]$, and aluminum nitrate nonahydrate$[Al(NO_3)_3 9H_2O]$ was used as the oxidizers, while urea (CH_4N_2O) was used as the fuel for the method. Europium oxide (Eu_2O_3) was used as the dopant precursor. All the reagents were obtained A.R. grade and taken according to their stoichiometric ratio.

The schematic of the synthesis process is shown in Fig. 1. 1. The precursor and initial reactant components were dissolved in double distilled water and combined using a porcelain mortar and pestle in a china dish. Later, the mixture was heated to 80 °C for 15-20 minutes to achieve a homogenous solution. The mixture was maintained at a temperature of about 525 °C in a preheated muffle furnace. As soon as the china dish was placed in the preheated furnace, the mixture boiled, triggering a breakdown process. This resulted in a combustion reaction in which combustible gases such as nitrogen oxides and ammonium oxides were liberated. The combustion process is accomplished quickly. The generated sample was foamy, and the foamy powder was removed immediately after the combustion process was completed. The frothy powder was crushed to a fine powder and sintered for four hours at 800 °C. The final produced product was subjected to characterisation, which was carried out at room temperature.

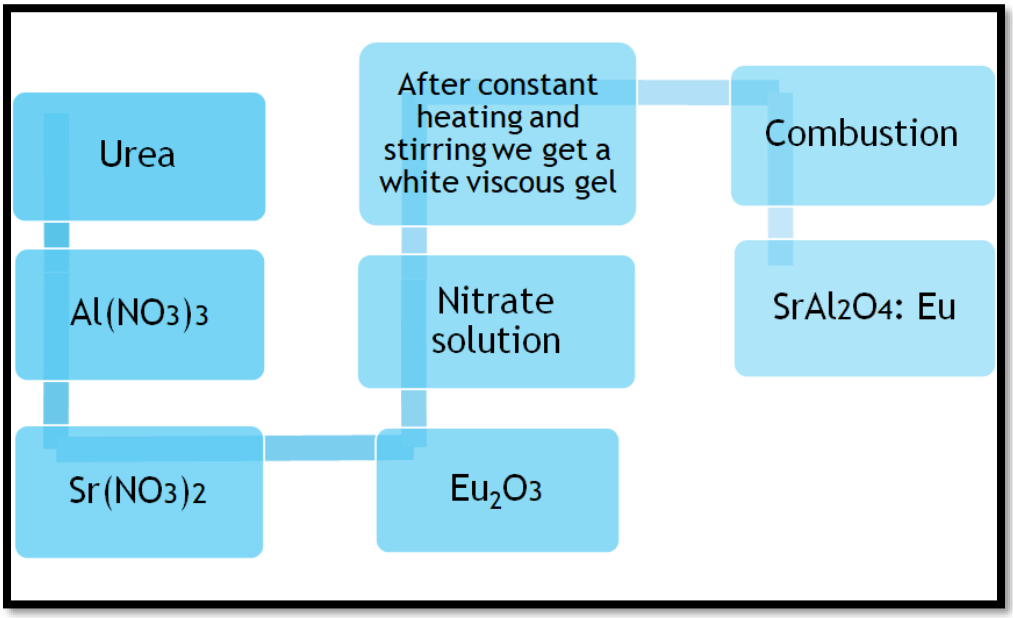

Fig. 1. 1 The schematic of the synthesis process SrAl2O4:Eu^{3+}

III. RESULTS AND DISCUSSION

X-RAY DIFFRACTION ANALYSIS

As seen by the XRD patterns (**Fig. 1. 2**), crystalline phase formation began at 800ºC with the formation of a phase with diffraction peaks suggesting the presence of monoclinic $SrAl_2O_4$ (JCPDS #34-0379). Additionally, X-ray diffraction patterns suggest that the different diffraction peaks at 2θ values of 20.00, 22.73, 29.27, 29.88, 31.97, 35.05, 40.69, 42.88, and 62.77 correspond to the (0 0 2), (0 1 2), (2 2 0), (1 2 1), (0 1 3), (2 1 0), (2 0 1), (2 0 2), (0 3 3) and (-1 0 7) plane The main peak at angle 2θ= 29.27º is the reflection of the crystallographic plane (220) for SrAl2O4. The XRD patterns of the annealed samples demonstrated a significant improvement in crystallinity, with more intense and sharper diffraction peaks. Additionally, the number of diffraction lines is increased in $SrAl_2O_4$ orientations when 800ºC annealing is used.

Scherrer's equation was used to calculate the crystal size of the sample based on the full width at half maximum (FWHM) of the most intense peak at 2θ=31.875º. The crystallite's average size was calculated to be approximately 35.34 nm. According to the literature, $SrAl_2O_4$ with filled tridymite–like structure belongs to the monoclinic P_{21} space group [9].

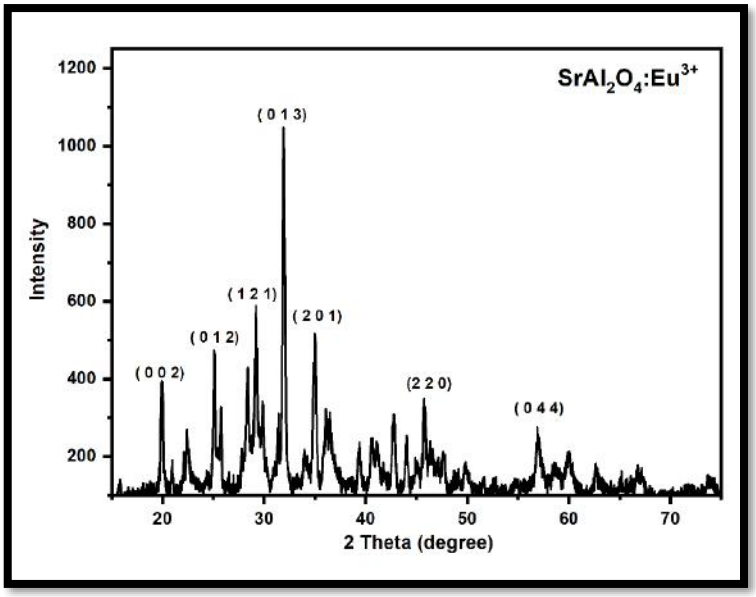

Fig. 1. 2 the XRD patterns $SrAl_2O_4$:2%Eu^{3+}

Table 1: Various parameters, i.e. Lattice constants (a), cell volume (V), X-ray density (X-ray) and crystallite size (D)

Lattice Constant					Volume (V) Å 3	X-ray density (ρ_x) g/cm^3	Molecular weight (M) gm/mole	Crystallite size (D) nm
a[Å]	b[Å]	c[Å]	α=γ	β				
5.209	8.5649	8.9113	90	93.65	396.77	3.44	205.54	35.34

FOURIER TRANSFORMATION INFRARED SPECTROSCOPY

Fig. 1. 3 shows the FT-IR spectra of $SrAl_2O_4$: Eu^{3+} powder. Due to the OH stretching vibrations of free and hydrogen-bonded hydroxyl groups, this spectrum reveals a broad band about 3433 cm^{-1}. However, a faint absorption band at 1632 cm^{-1} appears to be caused by the deformative vibration of water molecules, which is most likely caused by water absorption during the compaction of the powder specimens with KBr [11,12]. The appearance of a very weak band at 1382 cm^{-1} is owing to the N–O group's symmetric stretching vibrations, which may have been caused by the initial material's nitrate. Metal-oxygen stretching frequencies in the range 400–1000 cm^{-1} are related with Al–O, Sr–O, and Sr–O–Al bonding vibrations. A prominent peak at 846 cm1 was seen, which was attributed to the production of $SrAl_2O_4$ [13]

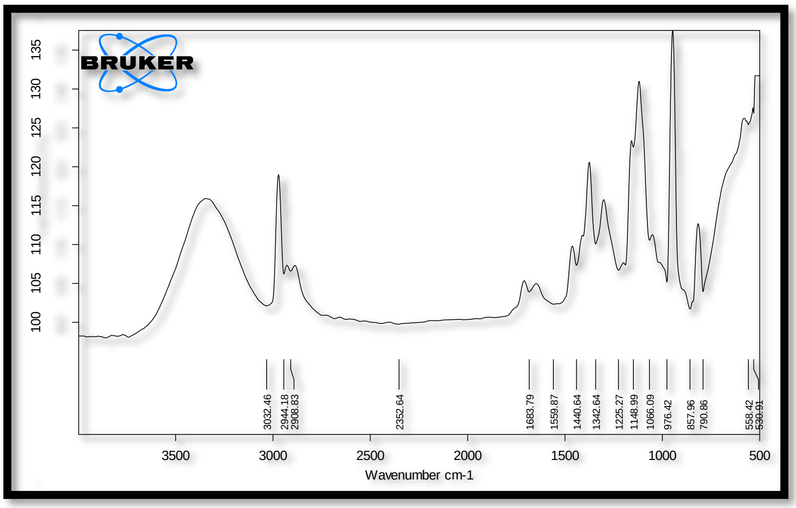

Fig. 1. 3 The FT-IR spectrum of $SrAl_2O_4$:2%Eu^{3+} powder

PHOTOLUMINESCENCE

Fig. 1. 4 shows excitation spectrum $SrAl_2O_4$: 2% Eu^{3+} was monitored at an emission wavelength of 616 nm and it exhibits a broad spectrum with peaks at around 394 and 466 nm, which correspond to transitions within the 4f6 configuration of Eu^{3+} ions [14]. **Error! Reference source not found.** Under 466 nm excitation, the apparent emission spectra of $SrAl_2O_4$: Eu^{3+} phosphor consists of many narrow and strong emission bands at 616 nm, as well as several minor emission bands. The major emission band should be defined as the transition from the splitting level $^5D_0 \rightarrow ^7F_2$ of Eu^{3+} to the splitting level $^5D_0 \rightarrow ^7F_j$ of Eu^{3+}. The emission spectrum must be identified as $^5D_0 \rightarrow ^7F_j$. The spectra associated with the transitions $^5D_0 \rightarrow ^7F_j$ are composed of several bands depending on the number of stark components in ^7F_j [15–17]. The 2J+1 rule governs the amount of stark components of Eu^{3+} in SrAl2O4 crystals. The transition $^5D_0 \rightarrow ^7F_2$ produces bands at 581, 588, 593, and 599 nm; transition $^5D_0 \rightarrow ^7F_2$ produces bands at 620 and 630 nm; and transition $^5D_0 \rightarrow ^7F_3$ produces bands at 650 and 658 nm [18,19]. At 615 nm, the hypersensitive band is due to the electric dipole transition $^5D_0 \rightarrow ^7F_2$ of Eu^{3+} ions.

The CIE chromaticity diagram of $SrAl_2O_4$:2%Eu^{3+} phosphors is shown in **Fig. 1. 5**. The CIE coordinates (0.5774, 0.4217) indicate red emission with a CCT of 1691 K and a CRI of 42. The CIE values of $SrAl_2O_4$:Eu^{3+} red phosphor is nearly identical to those of the commercial red-emitting phosphor Y_2O_3:Eu^{3+} [20,21].

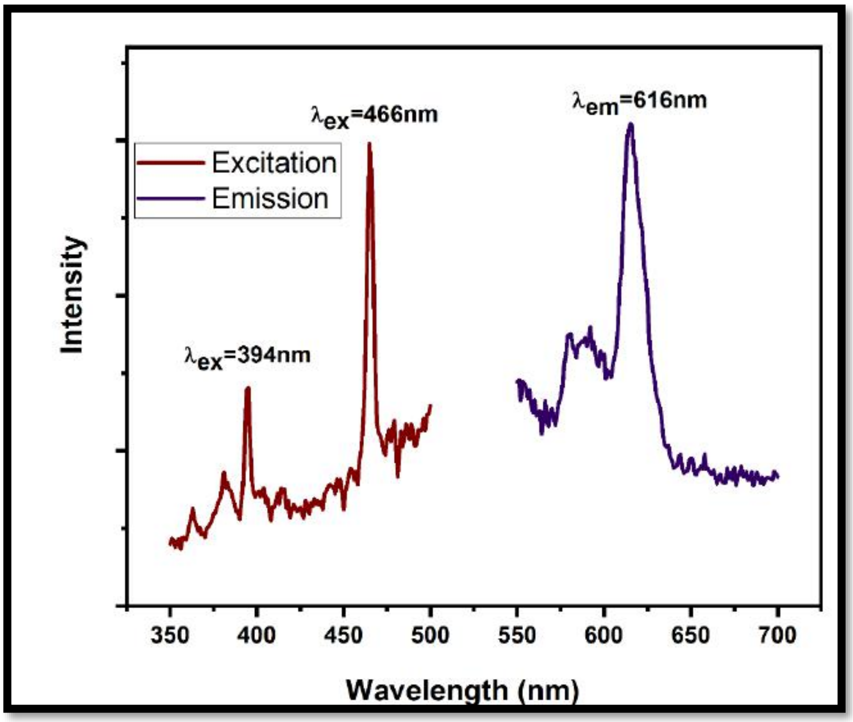

Fig. 1. 4 Photoluminescence graph of Europium doped $SrAl_2O_4$:2%Eu^{3+}

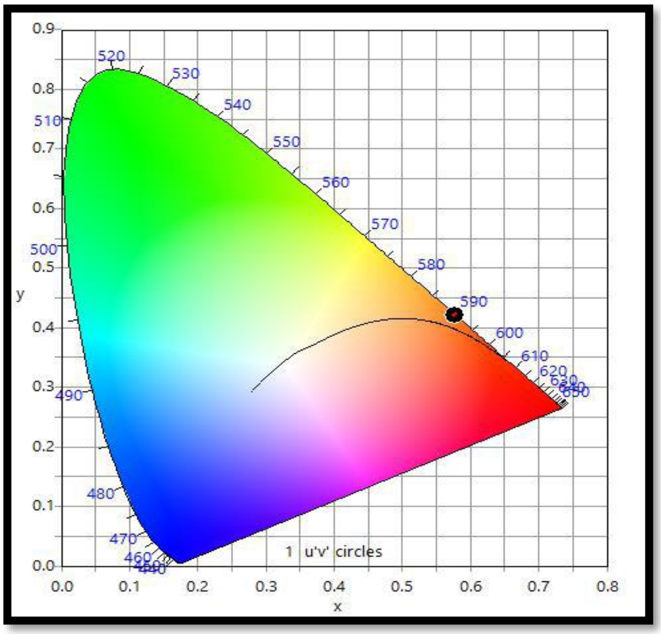

Fig. 1. 5 The CIE chromaticity diagram of $SrAl_2O_4$:2%Eu^{3+} phosphors

IV. CONCLUSION

Our results demonstrate that Eu is stabilised in the trivalent oxidation state in the produced SrAl2O4 phosphor. This phosphor might be generated in a short amount of time using the combustion process, resulting in a decrease in the rate of aluminate synthesis. X-ray Diffraction (XRD) was used to characterise the structural properties of annealed samples. Strontium aluminate samples were found to be monoclinic structure with a grain size of 35.34 nm as estimated by the Debye-Scherrer formula. FT-IR spectroscopy was used to confirm the vibrational stretching frequencies of the composites. The PL spectrum indicates that the highest emission occurs at 616 nm, which corresponds to the $^5D_0 \rightarrow {}^7F_2$ transition of Eu^{3+} ion, resulting in a bright red colour emitting phosphor used in display devices and lamp manufacturers. $SrAl_2O_4$: Eu^{3+} phosphors exhibit an orange-red emission band at 616 nm in their PL spectra. The CIE coordinates (0.5774, 0.4217) indicate red emission with a CCT of 1691 K and a CRI of 42.

REFERENCES

[1] V.B. Pawade, H.C. Swart, S.J. Dhoble, Review of rare earth activated blue emission phosphors prepared by combustion synthesis, Renewable and Sustainable Energy Reviews. 52 (2015) 596–612. https://doi.org/10.1016/j.rser.2015.07.170.

[2] D. Dutczak, T. Jüstel, C. Ronda, A. Meijerink, Eu^{2+} luminescence in strontium aluminates, Physical Chemistry Chemical Physics. 17 (2015) 15236–15249. https://doi.org/10.1039/c5cp01095k.

[3] K.A. Gedekar, S.P. Wankhede, S. v. Moharil, R.M. Belekar, Ce3+ and Eu2+ luminescence in calcium and strontium aluminates, Journal of Materials Science: Materials in Electronics. 29 (2018) 4466–4477. https://doi.org/10.1007/s10854-017-8394-0.

[4] H. Hagemann, J. Afshani, Synthesis, luminescence and persistent luminescence of europium-doped strontium aluminates, Handbook on the Physics and Chemistry of Rare Earths. (2021).

[5] R. Aroz, V. Lennikov, R. Cases, M.L. Sanjuán, E. Muñoz, G. F. de la Fuenta, Laser Synthesis and Luminescence Properties of SrAl2O4Eu2+,Dy3+ Phosphors, Physics Letters, Section A: General, Atomic and Solid State Physics. 381 (2017) 3519–3522.

[6] S. Singh, V. Tanwar, A.P. Simantilleke, D. Singh, Structural and photoluminescent investigations of SrAl2O4:Eu2+,RE3+ improved nanophosphors for solar cells, Nano-Structures and Nano-Objects. 21 (2020). https://doi.org/10.1016/j.nanoso.2020.100427.

[7] Y. Zhu, M. Ge, Study on the energy transfer ef fi ciency from SrAl 2 O 4 : Eu 2 þ , Dy 3 þ to light conversion agent of red-emitting phosphor : SrAl 2 O 4 : Eu 2 þ , Dy 3 þ / light conversion agent, 182 (2016) 173–176.

[8] V. Vitola, D. Millers, I. Bite, K. Smits, A. Spustaka, Recent progress in understanding the persistent luminescence in SrAl2O4:Eu,Dy, Materials Science and Technology (United Kingdom). 35 (2019) 1661–1677. https://doi.org/10.1080/02670836.2019.1649802.

[9] R. Neema, M. Saleem, P.K. Sharma, M. Mittal, Structure, optical bandgap and luminescence studies of SrAl2O4: Eu3+, Dy3+ nanophosphor, 3Rd International Conference on Condensed Matter and Applied Physics (Icc-2019). 2220 (2020) 020159. https://doi.org/10.1063/5.0002749.

[10] B. Liu, M. Gu, X. Liu, S. Huang, C. Ni, Theoretical study of structural, electronic, lattice dynamical and dielectric properties of SrAl2O4, Journal of Alloys and Compounds. 509 (2011) 4300–4303. https://doi.org/10.1016/j.jallcom.2011.01.046.

[11] K. Dev, A. Selot, G.B. Nair, V.L. Barai, N. Singh, F.Z. Haque, M. Aynyas, S.J. Dhoble, Study of luminescence properties of dysprosium-doped $CaAl_{12}O_{19}$ phosphor for white light-emitting diodes, Luminescence. 34 (2019) 804–811. https://doi.org/10.1002/bio.3675.

[12] V.B. Pawade, S.J. Dhoble, Novel blue-emitting $SrMg_2Al_{16}O_{27}$:Eu^{2+} phosphor for solid-state lighting., Luminescence : The Journal of Biological and Chemical Luminescence. 26 (2011) 722–727. https://doi.org/10.1002/bio.1304.

[13] T. Peng, L. Huajun, H. Yang, C. Yan, Synthesis of $SrAl_2O_4$:Eu, Dy phosphor nanometer powders by sol-gel processes and its optical properties, Materials Chemistry and Physics. 85 (2004) 68–72. https://doi.org/10.1016/j.matchemphys.2003.12.001.

[14] K. Mori, H. Onoda, T. Toyama, N. Osaka, Y. Kojima, Synthesis and fluorescence studies of Eu3+-doped SrAl12O19 phosphor, Optik. 180 (2019) 183–188. https://doi.org/10.1016/j.ijleo.2018.11.047.

[15] I.E. Kolesnikov, E. v. Golyeva, E.V. Borisov, E.Y. Kolesnikov, Photoluminescence properties of Eu3+-doped MgAl2O4 nanoparticles in various surrounding media, ChemInform. 40 (2009) 806–811. https://doi.org/10.1016/j.jre.2018.10.019.

[16] V. Sivakumar, U. v. Varadaraju, Synthesis, phase transition and photoluminescence studies on Eu3+-substituted double perovskites-A novel orange-red phosphor for solid-state lighting, Journal of Solid State Chemistry. 181 (2008) 3344–3351. https://doi.org/10.1016/j.jssc.2008.08.030.

[17] P. Chaware, A. Nande, S.J. Dhoble, K.G. Rewatkar, Structural, photoluminescence and Judd-Ofelt analysis of red-emitting Eu^{3+} doped strontium hexa-aluminate nanophosphors for lighting application, Optical Materials. 121 (2021) 111542. https://doi.org/10.1016/j.optmat.2021.111542.

[18] Y. Zhang, J. Xu, B.B. Yang, Q. Cui, T. Tian, Luminescence properties and energy migration mechanism of Eu3+ activated Bi4Si3O12 as a potential phosphor for white LEDs, Materials Research Express. 5 (2018) 26202. https://doi.org/10.1088/2053-1591/aaab8a.

[19] P. Halappa, S.T. Raj, R. Sairani, S. Joshi, R. Madhusudhana, C. Shivakumara, Combustion synthesis and characterisation of Eu3+-activated Y2O3red nanophosphors for display device applications, International Journal of Nanotechnology. 14 (2017) 833–844. https://doi.org/10.1504/IJNT.2017.086767.

[20] C.S. McCamy, Correlated color temperature as an explicit function of chromaticity coordinates, Color Research & Application. 17 (1992) 142–144. https://doi.org/10.1002/col.5080170211.

[21] X. Huang, Q. Sun, B. Devakumar, Preparation, crystal structure, and photoluminescence properties of high-brightness red-emitting Ca_2LuNbO_6:Eu^{3+} double-perovskite phosphors for high-CRI warm-white LEDs, Journal of Luminescence. 225 (2020) 117373. https://doi.org/10.1016/j.jlumin.2020.117373.